

## CHARACTERISTICS OF HEAT BALANCE DURING THE SNOWMELT SEASON IN NY-ÅLESUND, SPITSBERGEN ISLAND

Hironori NAKABAYASHI<sup>1</sup>, Yuji KODAMA<sup>2</sup>, Yukari TAKEUCHI<sup>3</sup>,  
Toshihiro OZEKI<sup>4</sup> and Nobuyoshi ISHIKAWA<sup>2</sup>

<sup>1</sup>*Japan Weather Association, Kita-4, Nishi-23, Chuo-ku, Sapporo 064*

<sup>2</sup>*Institute of Low Temperature Science, Hokkaido University, Kita-19, Nishi-8, Kita-ku, Sapporo 060*

<sup>3</sup>*Nagaoka Institute of Snow and Ice Studies, National Research Institute for Earth Science  
and Disaster Prevention, 187–16, Maeyama, Suyoshi-cho, Nagaoka 940*

<sup>4</sup>*Department of Civil Engineering, Faculty of Engineering, Hokkaido University, Kita-13, Nishi-8,  
Kita-ku, Sapporo 060*

**Abstract:** Heat balance observations were carried out at Ny-Ålesund, Spitsbergen Island during the snowmelt seasons in 1993 and 1994 in order to understand characteristics of heat balance at high latitude by comparing heat balance components at the snow surface before and after snowmelt initiation. In the snowmelt period, air temperature was higher than that in the pre-snowmelt period. Mean air temperature in the snowmelt period was about +3 ~ 4°C, and daily minimum temperature never fell below 0°C. Water vapor pressure was also higher than that in the pre-period. Albedo of the snow surface was relatively high, and remained higher than 0.65 even in the snowmelt period. The main snowmelt heat source was net radiation in both years. Net radiation in the snowmelt period was about 20 Wm<sup>-2</sup> larger than that in the pre-snowmelt period; however, the shortwave radiation budget was almost constant. Heat loss by the longwave radiation budget in the snowmelt period was less than that in the pre-period and consequently net radiation increased. The reason for the decrease of heat loss by the longwave radiation budget was the increase of atmospheric radiation accompanied by a decrease in solar radiation.

### 1. Introduction

Snowmelt is an important process for both the energy and water cycles. Snow has a high reflectivity to solar radiation and keeps the surface temperature at 0°C while it is melting, so a special atmospheric condition is generated over a snow-covered area compared to bare ground or a vegetated area. And melt water plays a great role in the annual water cycle in snowy regions. Especially in polar regions where seasonal snow melts in summer, snowmelt is also involved in glacier accumulation since the formation of superimposed ice at the interface of snow pack and glacier surface is caused by refreezing of snowmelt water.

On Spitsbergen Island (79°N, 12°E), about 60% of the surface is covered with glaciers and the rest with permafrost. The climate is mild compared to other high latitude regions due to the North Atlantic Current. The sun never falls below the horizon from late April to the middle of August (HISDAL *et al.*, 1992). Monthly mean air temperature in the warmest month (July) is about +5°C, and even in the coldest month (March) it is

about  $-12^{\circ}\text{C}$ . Annual precipitation is less than 400 mm (SAND *et al.*, 1991). Seasonal snow usually begins to melt early in June. Glacier accumulation mainly depends on superimposed ice, and it is important to understand the snowmelt process in considering the glacier mass balance. So heat balance observations were carried out at Ny-Ålesund, Spitsbergen Island during the snowmelt seasons in 1993 and 1994. The aim of this study is to investigate the heat balance characteristics and to clarify factors that control the snowmelt process in this region.

## 2. Observations

### 2.1. Observational site, periods and elements

Heat balance observations were carried out at Ny-Ålesund from the end of May to the middle of June in 1993 and 1994. A meteorological station was set up on flat tundra, about 2 km away from the terminus of Brøgger Glacier, and about 200 m inland from the shore of Kongsfjord (Fig. 1; modified from REPP, 1988).

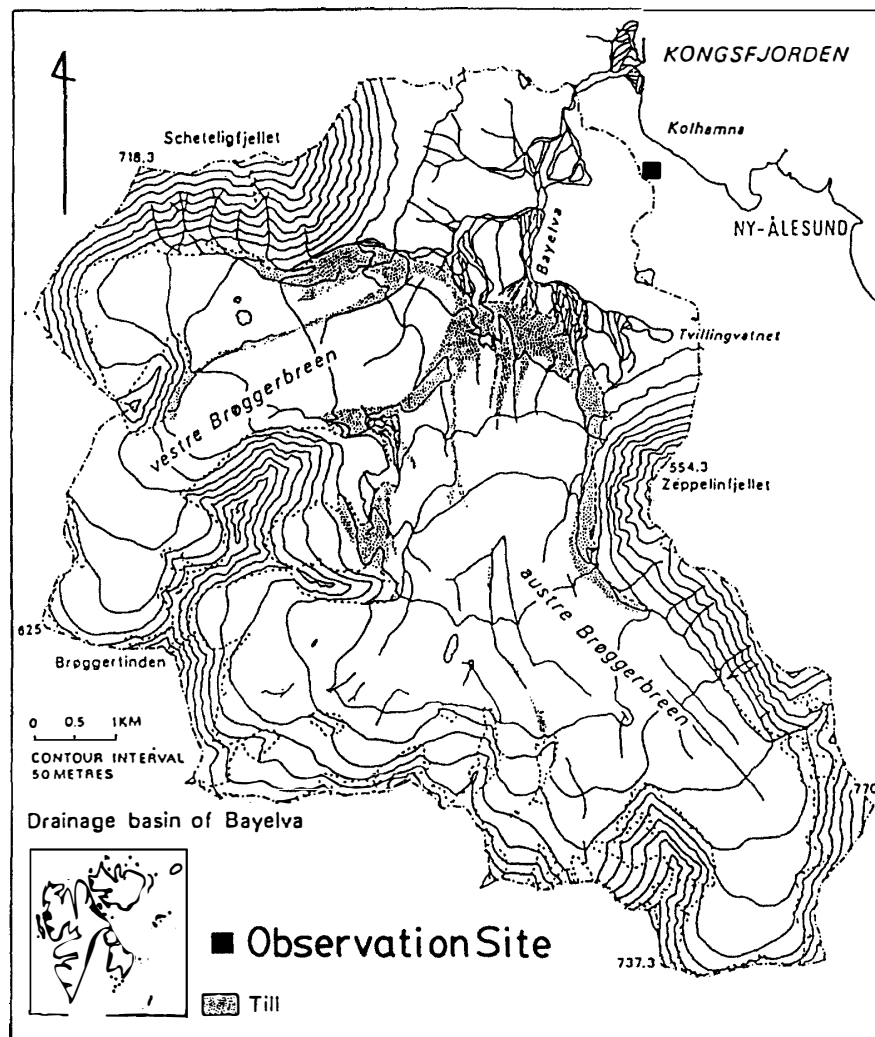


Fig. 1. The location map of the observation site (modified from REPP, 1988).

Table 1. Meteorological observation elements and instruments, measuring positions.

Elements	Instruments	Measuring positions
Air temperature	Hygrothermometer (Thermistor sensor)	100 cm above the snow surface
Relative humidity	Hygrothermometer (Static electrical capacity sensor)	"
Solar radiation	Pyranometer	"
Reflected solar radiation	Pyranometer (Albedo meter)	"
Atmospheric radiation	Infrared radiometer	"
Wind direction	Wind vane	"
Wind speed	Three cup type anemometer	"
Snow surface temperature	Infrared thermometer	20 cm above the snow surface
Snow temperature	Thermistor sensor	at 10 cm, 20 cm depth from the surface and at the bottom of snow pack in 1993, at 10 cm depth and at the bottom in 1994

Observed elements, instruments and measuring positions are listed in Table 1. Air temperature and relative humidity were measured with a thermistor sensor and static electrical capacity sensor mounted in a ventilated radiation shield. Wind speed and direction were measured with a three-cup type anemometer and wind vane, respectively. Solar radiation and reflected solar radiation were measured with two pyranometers, and atmospheric radiation was measured with an infrared radiometer. Snow surface temperature was measured with an infrared thermometer. All the equipment was set up 100 cm above the snow surface except for the infrared thermometer, which was set at 20 cm above the surface. Snow temperatures at the depths of 10 cm and 20 cm from the snow surface and at the bottom of the snow pack were measured in 1993. In 1994, basal ice about 10 cm thick existed under the snow pack at the observation site, and the temperatures at the depth of 10 cm and at the bottom (snow pack-basal ice interface) were measured. All meteorological elements were scanned every 30 s and recorded as 30 min mean values except for wind direction, which was recorded as an instantaneous value every 10 min.

During the observation periods in both years, weather conditions, cloudiness and cloud type were manually observed twice a day at 9 and 18 o'clock local time, and the heights and levels of all instruments were adjusted. Two snow stakes were set on the snow at the observation site, and snow depth was measured twice a day at 9 and 18 o'clock. At the same time, wet snow densities  $\rho_s$  ( $\text{kgm}^{-3}$ ) in layers 0–5 cm and 5–10 cm from the surface were obtained by a box type snow sampler.

## 2.2. Heat balance at the snow surface

The heat balance of the snow pack surface layer can be written as follows.

$$NR + QS + QL + QC + QM = 0, \quad (1)$$

where  $NR$  is the net radiation,  $QS$  the sensible heat flux,  $QL$  the latent heat flux,  $QC$  the

conductive heat flux in the snow pack and  $QM$  the heat for snowmelt. A positive sign of each flux represents heat flow into the snow pack, and negative heat flow away from it. When the snow temperature is below  $0^{\circ}\text{C}$ ,  $QM$  is the change of heat storage in the snow pack; negative  $QM$  means warming, and positive  $QM$  cooling. When the snow temperature is  $0^{\circ}\text{C}$ , negative  $QM$  is the heat used for snowmelt.

Net radiation is expressed with shortwave and longwave radiation terms.

$$\begin{aligned} NR &= SR - SU + AR - LU \\ &= SWRB + LWRB, \end{aligned} \quad (2)$$

where  $SR$  is the solar radiation,  $SU$  the reflected solar radiation,  $AR$  the atmospheric radiation, and  $LU$  the longwave upward radiation, which is defined here as the black body radiation at the snow surface temperature.  $SWRB$  and  $LWRB$  are the net shortwave and longwave radiation, respectively. Total net radiation is obtained by directly measuring the terms on the right hand side of eq. (2). Sensible and latent heat fluxes are derived by using a bulk method expressed as eqs. (3) and (4), respectively.

$$QS = \rho_a Cp Kh(AT - ST)WS, \quad (3)$$

$$QL = \rho_a LKe(Aq - Sq)WS, \quad (4)$$

where  $\rho_a$  is the air density,  $Cp$  the specific heat at constant pressure, and  $AT$ ,  $Aq$  and  $WS$  are air temperature, specific humidity, and wind speed at the height of 100 cm above the snow surface, respectively.  $L$  is the latent heat of vaporization.  $ST$  and  $Sq$  are temperature and specific humidity at the snow surface.  $Sq$  is considered as the saturated value at the snow surface temperature.  $Kh$  and  $Ke$  are the bulk transport coefficients for sensible and latent heat, respectively. After MALE and GRANGER (1981), both coefficients are equivalent under stable condition. During the observation periods, air temperature was always higher than that of the snow surface (TAKEUCHI *et al.*, 1995), and it can be assumed that the atmosphere near the snow surface was in stable condition. The value of  $Kh$  used in this study is  $2.2 \times 10^{-3}$  for smooth snow surface (TAKEUCHI and KONDO, 1981). Conductive heat flux in the snow pack is proportional to the snow temperature gradient, and it is written as follows.

$$QC = \lambda (T1 - T2)/\Delta Z, \quad (5)$$

where  $T1$  and  $T2$  are the snow temperatures at different depths,  $\Delta Z(\text{m})$  is the distance between them, and  $\lambda$  ( $\text{WK}^{-1}\text{m}^{-1}$ ) is the heat conductivity of the snow pack expressed as a function of snow density  $\rho_s$  ( $\text{kgm}^{-3}$ ) (AKITAYA, 1974).

$$\log_{10}(4.18 \times 10^2 \lambda) = -3.6 + 1.8 \times 10^{-3} \rho_s. \quad (6)$$

Heat for snowmelt ( $QM$ ) can be derived as the residual of eq. (1).

To confirm the heat balance calculation, snowmelt energy is compared to the snow-

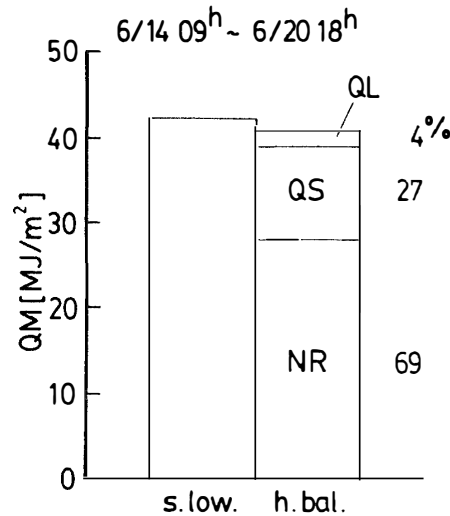


Fig. 2. Comparison of snowmelt energies between the surface lowering (s.low.) method and the heat balance (h.bal.) method in 1993 (from NAKABAYASHI *et al.*, 1994).

melt amount in 1993 (NAKABAYASHI *et al.*, 1994). Figure 2 shows the snowmelt energies calculated from different methods. In Fig. 2, “s.low.” means the snowmelt energy calculated from snowmelt amount  $\Delta M$  ( $\text{kgm}^{-2}$ ), which is obtained as a product of the wet snow density at the surface  $\rho_s$  ( $\text{kgm}^{-3}$ ) and the snow “surface lowering”  $\Delta h$  (m) (ISHIKAWA *et al.*, 1985),

$$\Delta M = \rho_s \Delta h, \quad (7)$$

and “h.bal.”, from the “heat balance” calculation. In the snowmelt season, temperature of the entire snow pack stays at  $0^\circ\text{C}$ , so the conductive heat flux ( $QC$ ) was eliminated, and eq. (1) is simplified to eq. (8).

$$NR + QS + QL + QM = 0, \quad (8)$$

The two energies coincide well; however, the snowmelt energy calculated from snowmelt amount (s.low.) is slightly larger than that from the heat balance calculation.

### 3. Results and Discussion

Figure 3 shows the snow depth during the observation periods in 1993 and 1994. In early June 1993, snow depth remained relatively constant between 41 and 46 cm, and large surface lowering was observed on June 14. After that, snow depth decreased monotonously until snow disappeared on June 21. In 1994, snow depth was less than in 1993, and surface lowering began gradually from June 10. In this year, basal ice about 10 cm thick existed under the snow pack.

Figures 4a and 4b show the snow temperatures at different depths from the snow surface in 1993 and 1994, respectively. Temperatures in the upper part of the snow pack

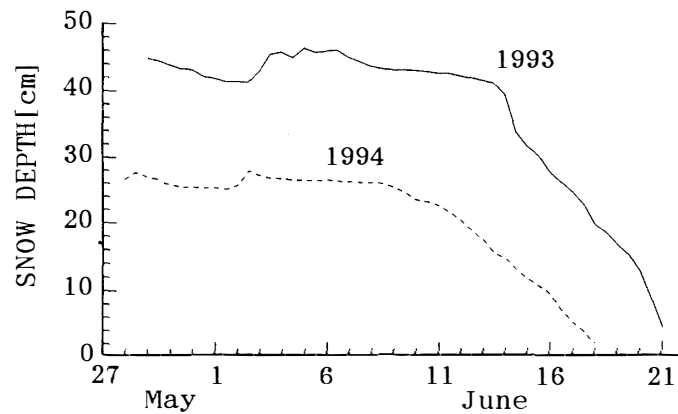


Fig. 3. Snow depth measured twice a day at 9 and 18 o'clock at the observation site during the observation period in 1993 and 1994.

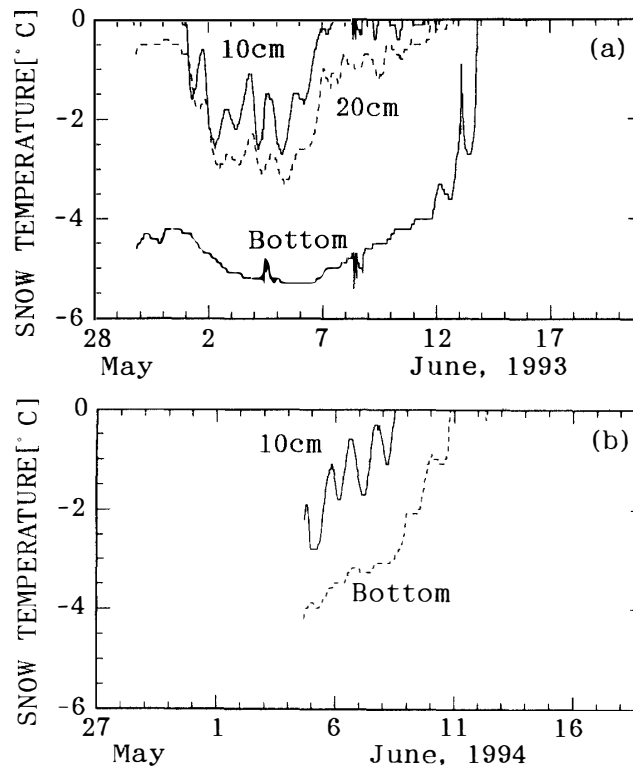


Fig. 4. Snow temperatures at different depths from the snow surface. (a) at the depth of 10 cm and 20 cm from the snow surface and at the bottom of snow pack in 1993. (b) at the depth of 10 cm and at the bottom (snow-basal ice interface) in 1994.

were higher than those of the lower part. In early June, the temperature at the bottom of snow pack was about  $-4 \sim -5^{\circ}\text{C}$ , and rose day by day, reaching  $0^{\circ}\text{C}$  on June 13 in 1993, June 10 in 1994. The remarkable decrease of snow depth began just after the temperature at the bottom reached  $0^{\circ}\text{C}$  in both years. After that, the temperature of whole snow pack remained at  $0^{\circ}\text{C}$ .

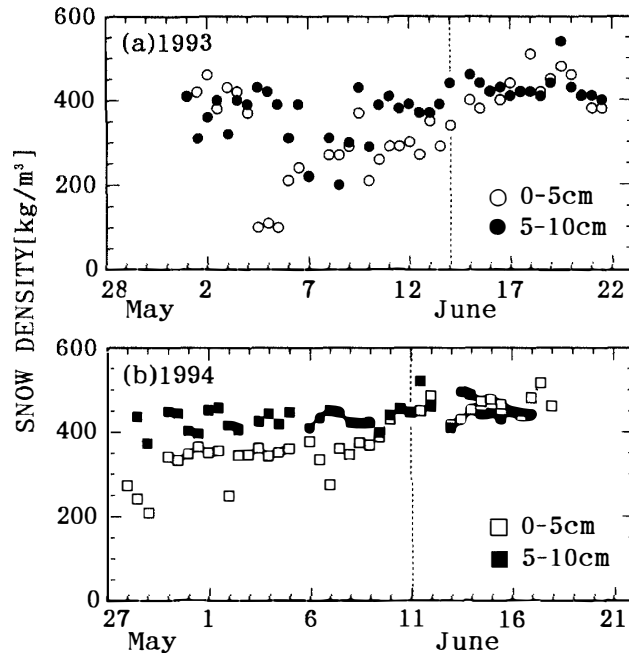


Fig. 5. Snow densities in two different layers (0–5 cm and 5–10 cm from the snow surface). (a) 1993, (b) 1994.

Figures 5a and 5b show the snow densities in layers 0–5 cm and 5–10 cm from the surface in 1993 and 1994, respectively. After the snow temperature reached  $0^{\circ}\text{C}$ , the difference of density in the two layers became smaller and maintained almost constant values of about  $420\text{--}430\text{ kg m}^{-3}$  until the snow disappeared. Snow density of the entire snow pack was measured on June 15 in 1993 and June 8 in 1994; the values were  $430$  and  $330\text{ kg m}^{-3}$  for 1993 and 1994, respectively. Therefore, the surface lowering after the snow temperature reached  $0^{\circ}\text{C}$  was considered to be due to snowmelt, not densification in 1993, but in 1994, surface lowering was due to not only snowmelt but densification.

In this study, the period before the snow temperature reached  $0^{\circ}\text{C}$ , *i.e.* until June 13 in 1993 and June 10 in 1994, is defined as the pre-snowmelt period, and the period from that date to snow disappearance is defined as the snowmelt period. Heat balance characteristics before and after snowmelt initiation will be discussed in the following sections. Melting of the basal ice in 1994 is not discussed in this paper.

### 3.1. Meteorological elements before and after snowmelt initiation

Figures 6a–c show daily extremes and means of air temperature, water vapor pressure and wind speed in 1993, respectively. Figures 7a–c are the same as Fig. 6 but in 1994. Air temperatures in the snowmelt period were higher than those of the pre-snowmelt period in both years. During the snowmelt period, mean air temperature was about  $+3\text{--}4^{\circ}\text{C}$ , and minimum temperature never fell below  $0^{\circ}\text{C}$ . Water vapor pressure in the snowmelt period was also higher by 1–2 hPa than that in the pre-snowmelt period. Although not shown here, air temperature and water vapor pressure show diurnal patterns in phase. Note that the sun was above the horizon all day long during the observation period. Daily ranges of air temperature and water vapor pressure were larger on clear

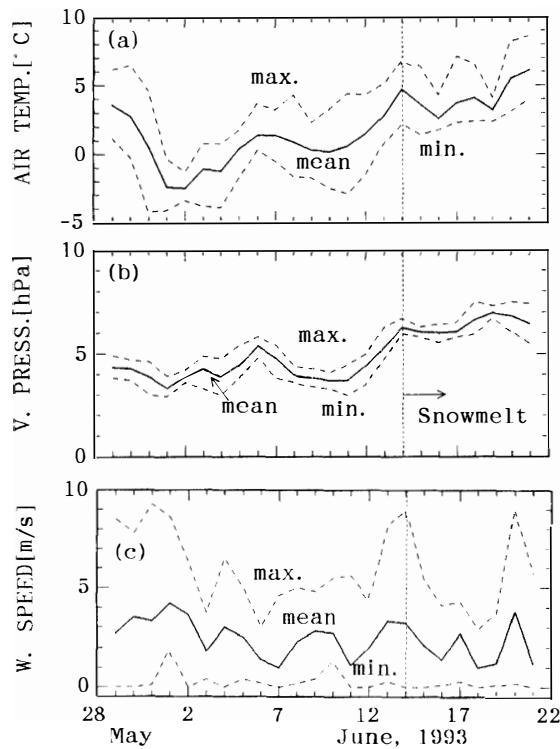


Fig. 6. The daily extremes and mean values of meteorological elements in 1993. (a) air temperature, (b) water vapor pressure, (c) wind speed.

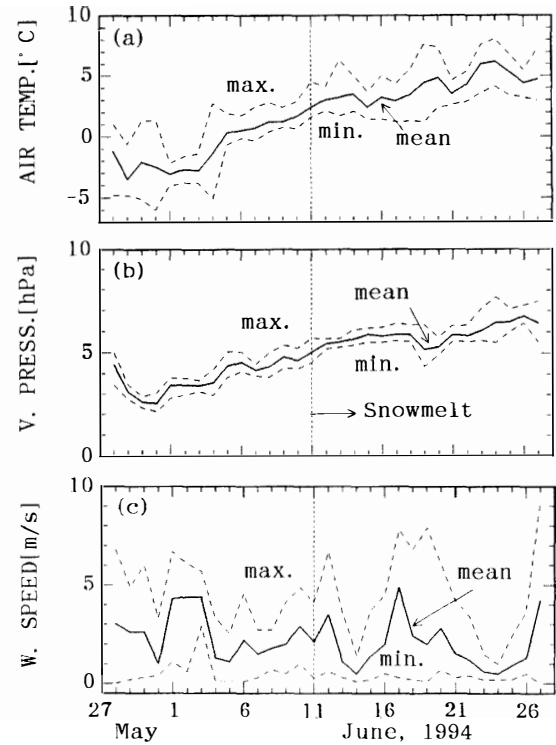


Fig. 7. The same as Fig. 6 but in 1994.

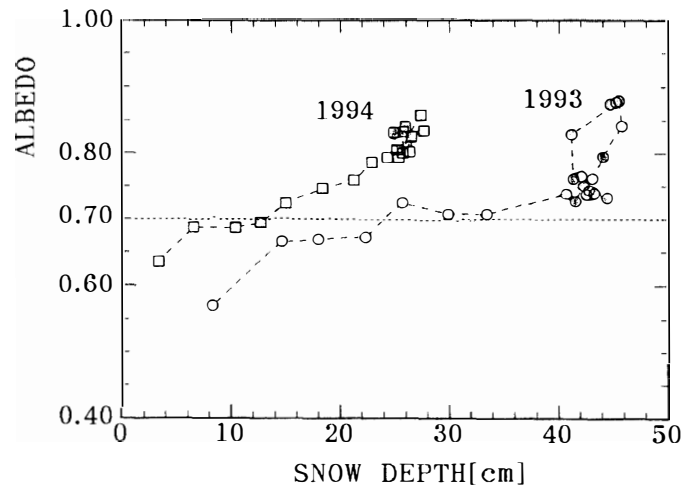


Fig. 8. The relation between snow depth and snow surface albedo in 1993 and 1994.

days than cloudy or rainy days. For wind speed, there was no clear diurnal variation or systematic change in the observation period.

Figure 8 shows the relation between snow depth and snow surface albedo in 1993 and 1994. At the beginning of the observation period, albedo ranged from 0.75 to 0.85,



and decreased gradually with decreasing snow depth, *i.e.* progress of snowmelt, but it remained higher than 0.65 even in the snowmelt period. From Fig. 8, it can be seen that snowmelt occurs when the albedo is about 0.7 in both years.

### 3.2. Comparison of heat balance components

Figures 9a and 9b show the daily accumulated values of net radiation (*NR*), sensible heat flux (*QS*), latent heat flux (*QL*) and conductive heat flux in the snow pack (*QC*) for seven days in the pre-snowmelt period and for six days in the snowmelt period in 1993 and 1994, respectively. There was no remarkable difference in sensible heat flux through the observation period, and the sign was always positive. This means that air temperature was always higher than that of the snow surface, and sensible heat flux was transported to the snow pack. Conductive heat flux has a negative sign; this means that the lower part of the snow pack was warmed by the conductive heat flux. In the snowmelt period, the entire snow pack was isothermal at 0°C; therefore, the conductive heat flux became zero. The negative sign of latent heat flux means evaporation from the snow surface, and positive means condensation on to the surface. For both years, evaporation occurred in the pre-snowmelt period, and evaporation amount decreased in the snowmelt period due to the increase of water vapor in the atmosphere. In the snowmelt period in 1993, latent heat flux became positive, *i.e.* condensation occurred, but the quantity of energy was small. Among the heat balance components, net radiation increased greatly from the pre-snowmelt period to the snowmelt period, and became the largest heat source

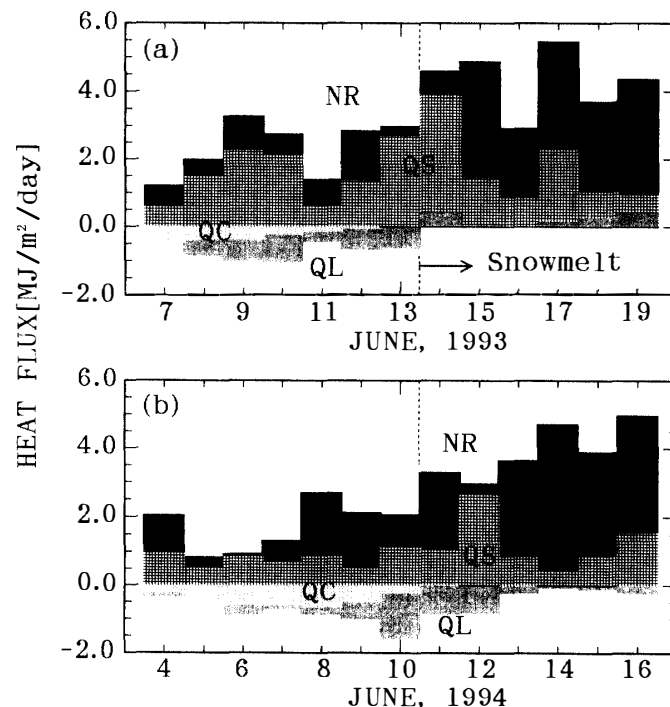


Fig. 9. Heat balance components expressed as daily accumulated values for seven days before snowmelt initiation and six days after that in 1993(a) and 1994(b). NR: net radiation, QS: sensible heat flux, QL: latent heat flux and QC: conductive heat flux.

for snowmelt in both years (70% of  $QM$  or more). In the next section, reasons for the increase of net radiation will be discussed.

### 3.3. Characteristics of net radiation

Figure 10 shows the relation between daily mean shortwave radiation budget ( $SWRB$ ) and daily mean longwave radiation budget ( $LWRB$ ) in 1993 (circles) and 1994 (squares). Hollow marks are for the pre-snowmelt period and solid ones are for the snowmelt period.  $SWRB$  is the difference between solar radiation and reflected solar radiation.  $LWRB$  is the difference between atmospheric radiation and terrestrial radiation. The terrestrial radiation is obtained here as the black body radiation at the snow surface temperature. From Fig. 10, the larger  $LWRB$  in the snowmelt period can be seen when it is compared with the one in the pre-snowmelt period for the same  $SWRB$ . The variation of  $SWRB$  is mainly due to the cloudiness because the albedo of the snow surface was relatively constant (Fig. 8), and there was no systematic change in  $SWRB$  from the pre-snowmelt period to the snowmelt period. The  $LWRB$  is negative in almost the whole observation period, which means heat loss from the snow surface. The larger  $LWRB$  found in the snowmelt period means smaller heat loss from the snow surface. Since the longwave upward radiation increases from the pre-snowmelt period to the snowmelt period because the snow surface temperature rises to  $0^{\circ}\text{C}$  (273 K), the increase in  $LWRB$  must be due to the increase in atmospheric radiation, which depends on air temperature, water vapor content in the atmosphere and cloudiness (*e.g.* SUGITA and BRUTSAERT, 1993). In the next paragraph, the changes of solar radiation and atmospheric radiation are discussed.

Figures 11a and 11b show the variations in daily mean solar radiation ( $SR$ ) and atmospheric radiation ( $AR$ ) during the observation periods in 1993 and 1994, respec-

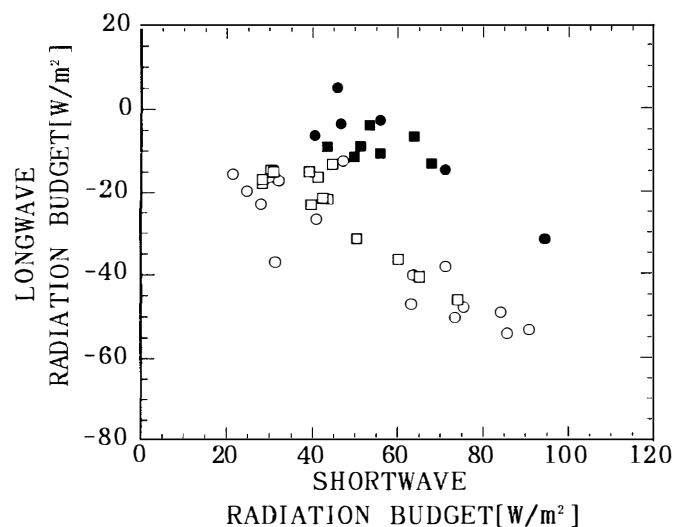


Fig. 10. The relation between the daily mean shortwave radiation budget ( $SWRB$ ) and longwave radiation budget ( $LWRB$ ) in 1993 and 1994. Circles represent the relation in 1993 and squares in 1994. Hollow and solid marks represent the relation during the pre-snowmelt period and the snowmelt period, respectively.

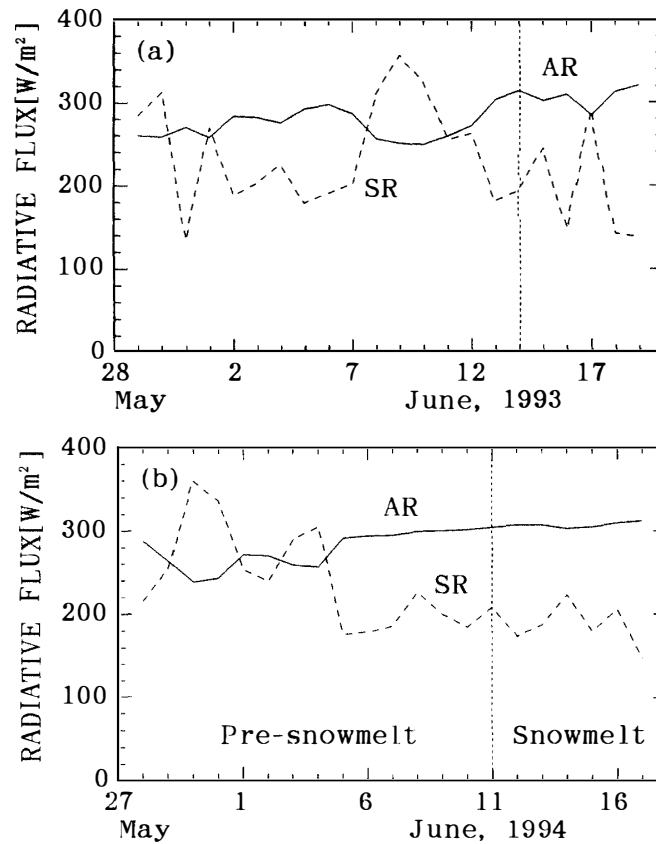


Fig. 11. The variations of daily mean solar radiation (*SR*) and atmospheric radiation (*AR*) during the observation periods in 1993 (a) and 1994 (b).

tively. *SR* did not show systematic change before and after the initiation of snowmelt; however, the increase of *AR* is clearly seen. Especially in 1993, *AR* increased and *SR* decreased from 2 to 3 days before the initiation of snowmelt. In 1994, *AR* increased gradually; however, the decrease in *SR* is obvious. Figures 11a, b also show the negative correlation between *AR* and *SR*. A increase of *AR* accompanied a decrease of *SR*.

As mentioned before, the variation of *SR* is mainly due to cloudiness. Increase of cloudiness occurs with decrease in *SR* and also increase of *AR*. The increase in *AR* is accompanied by rising air temperature and water vapor pressure. Although it is difficult to conclude from the results of the two years of observations, this phenomenon seems to occur due to warm and moist air advection from lower latitude (NAKABAYASHI *et al.*, 1994).

As we have previously seen, the main heat source for snowmelt is net radiation. The increase of net radiation from the pre-snowmelt to the snowmelt period is the increase in *LWRB*, although the largest component in net radiation is *SWRB*. The increase in *LWRB* (decrease in longwave heat loss) is mainly due to the increase in *AR*, which is accompanied by a decrease in *SR*. That is, the initiation of snowmelt is accompanied by the increase of *AR*; however, the main heat source for snowmelt is *SR*.

#### 4. Summary and Conclusions

Heat balance observations were carried out at Ny-Ålesund, Spitsbergen during the snowmelt seasons in 1993 and 1994, and heat balance characteristics at high latitude were investigated. The main snowmelt heat source was net radiation in both years. In the snowmelt period, net radiation increased; however, the shortwave radiation budget did not change systematically. The heat loss by net longwave radiation in the snowmelt period was less than that in the pre-snowmelt period, and net radiation increased. The decrease of heat loss by net longwave radiation is mainly due to an increase of atmospheric radiation accompanied by a decrease in solar radiation.

#### Acknowledgments

Our thanks go to Drs. S. USHIO and S. KUDOH, National Institute of Polar Research, without whose help these measurements could not have been taken. A part of this research was supported by a scientific research grant from the Ministry of Education, Culture, Sports and Science of Japan (No. 05041069, No. 05044065).

#### References

- AKITAYA, E. (1974): Studies of depth hoar. *Contrib. Inst. Low Temp. Sci., A*, **26**, 67 p.
- HISDAL, V., FINNEKÅSA, Ø. and VINJE, T. (1992): Radiation Measurements in Ny-Ålesund, Spitsbergen 1981–1987. Norsk Polarinstitutt, 380 p.
- ISHIKAWA, N., KOJIMA, K. and MOTOYAMA, H. (1985): Prediction of hourly and daily amounts of snowmelt by heat balance or bulk meteorological elements. *Teion Kagaku, Butsuri-hen (Low Temp. Sci., Ser. A, Phys.)*, **44**, 63–75 (in Japanese with English abstract).
- MALE, D.H. and GRANGER, R.J. (1981): Snow surface energy exchange. *Water Resour. Res.*, **17**, 609–627.
- NAKABAYASHI, H., KODAMA, Y. and TAKEUCHI, Y. (1994): Process of snowmelt in Spitsbergen. *Teion Kagaku, Butsuri-hen (Low Temp. Sci., Ser. A, Phys.)*, **53**, 11–22 (in Japanese with English abstract).
- REPP, K. (1988): The hydrology of Bayelva, Spitsbergen. *Nordic Hydrol.*, **19**, 259–268.
- SAND, K., HAGEN, J.O., REPP, K. and BERNTSEN, E. (1991): Climate related research in Svalbard. *Norw. Nat. Comm. Hydrol. Rep.*, **23**, 203–217.
- SUGITA, M. and BRUTSAERT, W. (1993): Cloud effect in the estimation of instantaneous downward longwave radiation. *Water Resour. Res.*, **29**, 599–605.
- TAKEUCHI, K. and KONDO, J. (1981): *Taiki Kagaku Kôza 1 Chihyo ni Chikai Taiki (Lectures on Atmospheric Science 1 Atmosphere near the Ground)*. Tokyo, Univ. Tokyo Press., 226 p.
- TAKEUCHI, Y., KODAMA, Y. and NAKABAYASHI, H. (1995): Characteristics of evaporation from snow and tundra surface in Spitsbergen in snowmelt season 1993. *Proc. NIPR Symp. Polar Meteorol. Glaciol.*, **9**, 54–65.

*(Received November 1, 1995; Revised manuscript accepted March 21, 1996)*